

Development of Laser-Based Diagnostics to Measure Aerosol Optical Properties

Chad C. Schmidt*, Manvendra K. Dubey, John R. Stephens
Los Alamos National Laboratory, Los Alamos, NM 87545

* chads@lanl.gov, 505 667-7999

Introduction

Aerosols play a key but complex role in the global energy budget and atmospheric chemistry. They directly scatter and absorb incoming solar radiation. They indirectly affect cloud properties which control both the reflected short-wave and trapped long-wave terrestrial radiation. The IPCC-95 report places "very low" confidence levels on our understanding of aerosols and states that "the cooling due to aerosols should not necessarily be regarded as an offset against the greenhouse gas warming." This report also cites the largest uncertainties in direct radiative forcing arising from two sources:

- The poorly known scattering efficiencies of sulfate aerosols as a function of relative humidity.
- The absence of information on the optical properties of particles containing soot, mineral dust, and organics.

The goal of this work is to enhance our confidence in climate assessments by quantifying the contribution of aerosols and clouds to the earth's radiation budget by measuring absorption and scattering cross-sections of single aerosols at solar and infrared wavelengths.

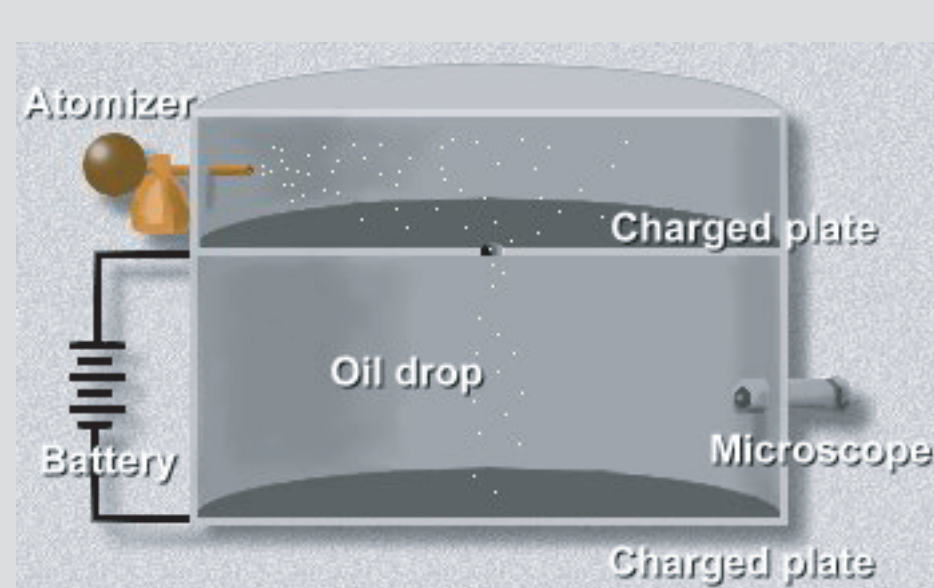


Smog over Seattle commuters.

1

The Electrodynamic Balance Facility

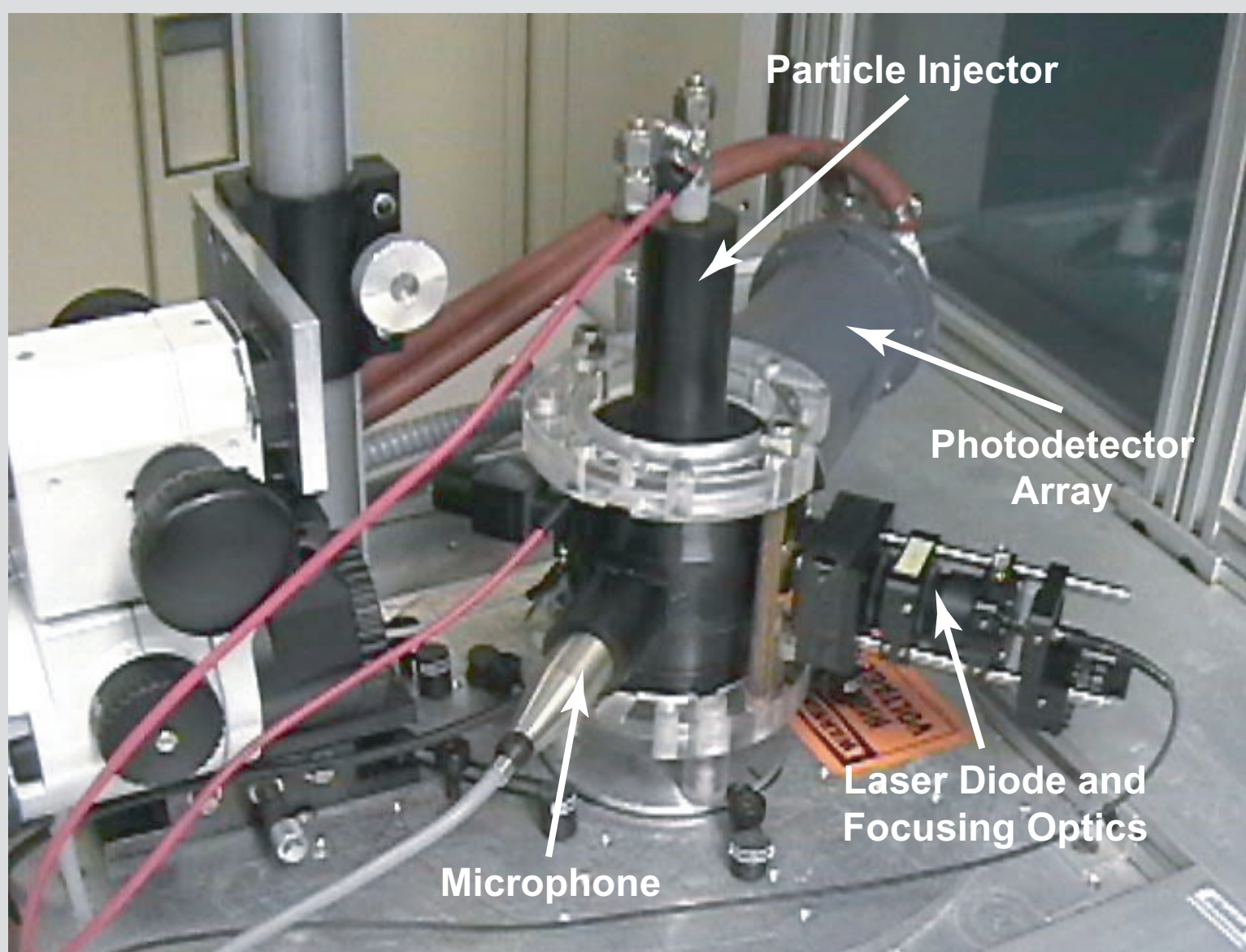
The Electrodynamic Balance Facility (EDB) is based on the classical Millikan oil drop experiment of 1909. The EDB is used to isolate a single charged particle in an electric field. The EDB configuration used in this work is a bihyperloidal balance. This configuration consists of two end electrodes and a center torus, all with hyperbolic cross-sections. A number of charged particles are introduced into the EDB through the top electrode and become suspended in the AC field applied to the center electrode. A symmetric DC potential is applied to the end electrodes to both eject particles from and focus the remaining particle at the center of the EDB. The DC potential provides an offset to gravitational forces and provides a measure of the charge to mass ratio of the particle. Using the EDB, a single particle can be trapped and held for a period of weeks, allowing for a number of diagnostics to be employed on the same particle. The facility used in this work is also equipped with controls for temperature, pressure, and bulk gas composition so that a variety of atmospheric conditions may be simulated.



The Millikan Oil Drop Experiment.

2

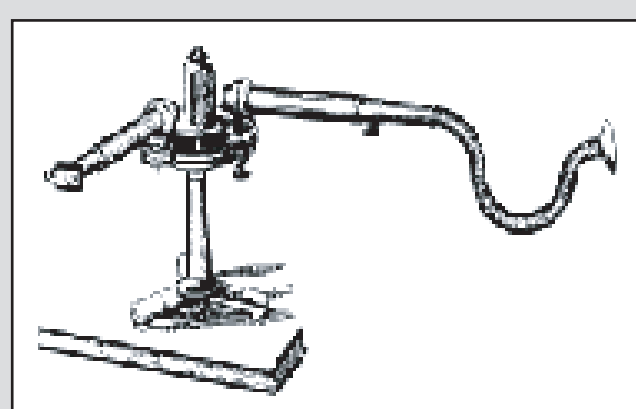
The Electrodynamic Balance Facility



3

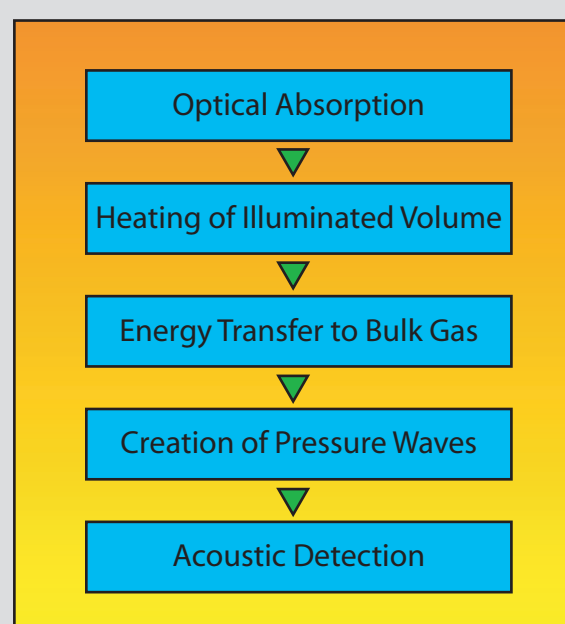
Photoacoustic Spectroscopy

Photoacoustics is the production of acoustic waves by the absorption of light. The history of the photoacoustic effect dates back to 1880 when Alexander Graham Bell first observed it while working on a way to transmit sound without any cables. The invention of the microphone 50 years later made it possible to enhance the measurements and in 1973 a detailed model of the effect was developed by Rosenzweig and Gersho.



Alexander Graham Bell's photophone.

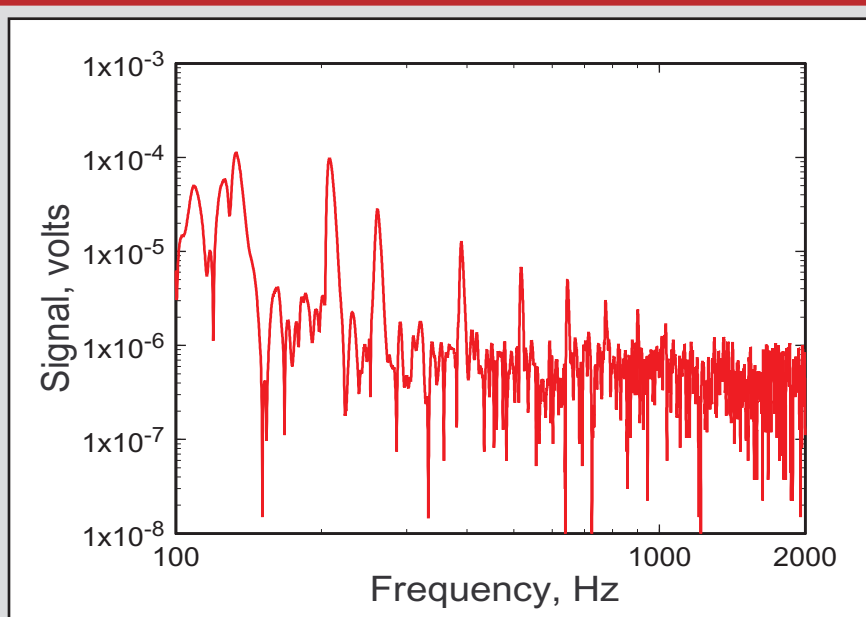
Evolution of the photoacoustic signal.



Photoacoustic signal is produced by periodic excitation of an absorbing sample. The sample absorbs energy and transfers that energy as heat to the background gas. The heating of the background gas produces pressure waves that can be detected with a sensitive microphone. To strengthen the photoacoustic signal, modulation of the excitation source at the resonant frequency of the sample cell and lock-in detection are commonly used. The EDB facility in this work also allows for particle modulation rather than excitation source modulation.

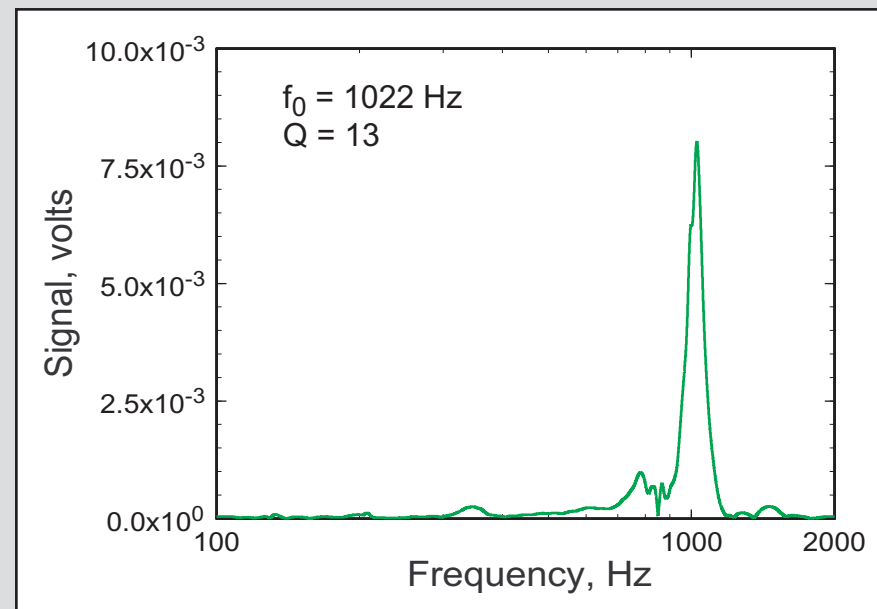
4

Characterization of the Acoustic Noise



Measurement of the room noise.

The photoacoustic signal can be amplified by operating at a resonant mode of the EDB. To detect the resonant frequency of the EDB, a speaker was placed in the acoustic enclosure and swept through a range of frequencies. The figure to the right shows a resonant mode at 1022 Hz. The quality factor, Q, can also be computed from this data. Comparison of these two figures shows that resonance occurs where room noise is low.

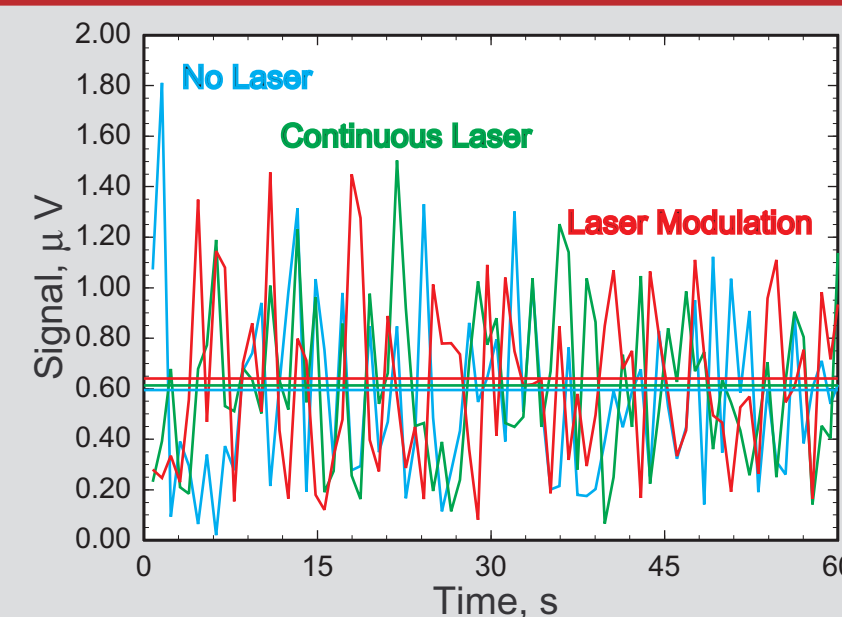


Measurement of the Quality Factor.

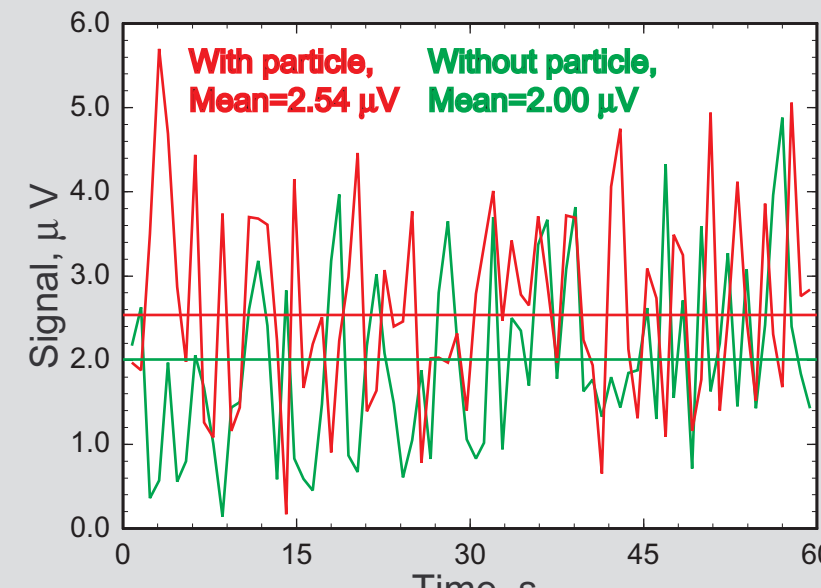
5

Photoacoustic Signal from a Particle

When the light source is modulated, photoacoustic signal may be generated from heating of windows, walls, and bulk gas. The EDB can be used to instead modulate the particle through the path of a continuous excitation source, eliminating this noise. The figure at right shows there is only a 5% increase in the noise due to modulation of the light source relative to a continuous laser. Solid lines represent the mean signal. Since the increase in noise from laser modulation is minimal, laser modulation is used for all photoacoustic experiments.



Effect of laser modulation on the background noise - no particle in the EDB.

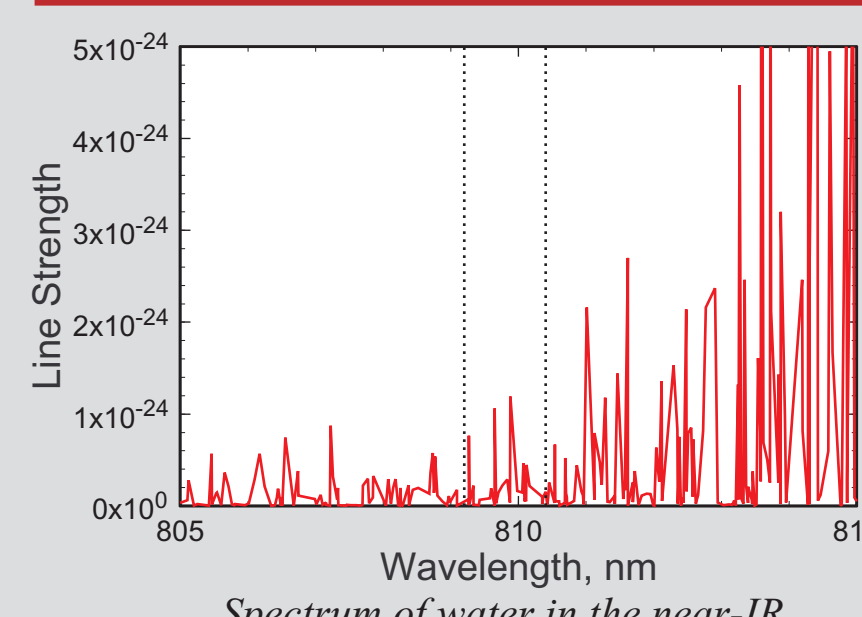


Photoacoustic signal from a single particle.

The figure to the left shows the photoacoustic signal due to a 10 μm sphere dyed to absorb at 810 nm. The signal with a particle in the EDB is 25% higher than without a particle. The laser power for this experiment was approximately 100 mW. Solid lines again represent the mean signal. Excitation frequency was at the resonant frequency of the EDB. It is believed that with further reduction of the background noise, signal to noise ratios of up to 4 can be achieved.

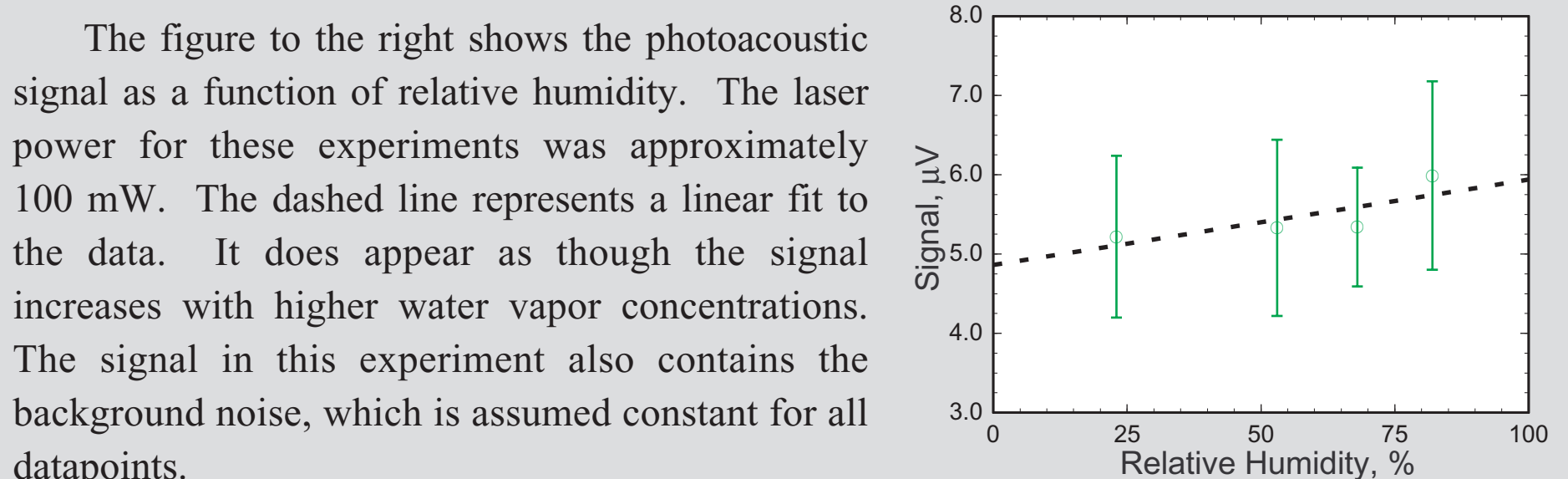
6

Gas Phase Photoacoustic



Spectrum of water in the near-IR.

To establish the sensitivity of the photoacoustic technique and begin looking for ways to calibrate the absorbance versus photoacoustic signal, gas phase measurements of water vapor were performed. The setup for this experiment is not ideal since the 810 nm laser only overlaps weak absorption features in the water near-IR spectrum- see figure at left.

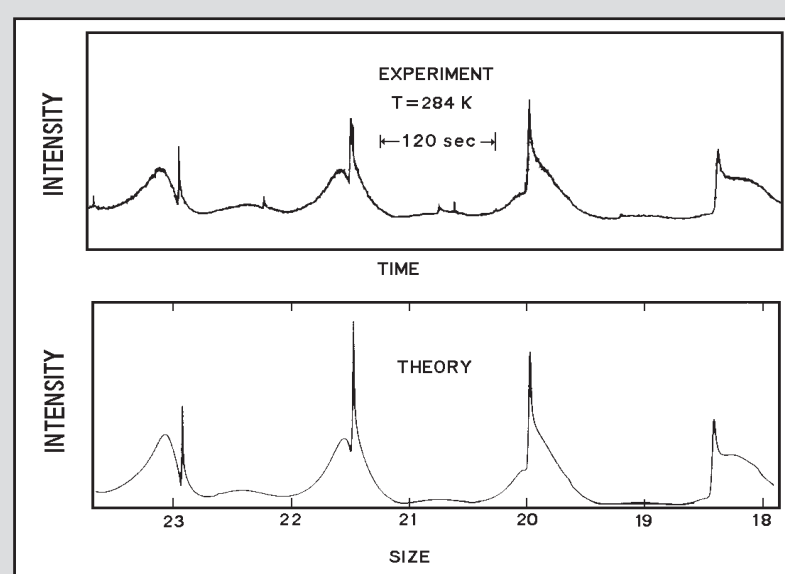


Photoacoustic signal versus Relative Humidity

7

Particle Sizing Technique

Mie theory is the foundation for two popular methods of determining the size of a single particle or droplet. The first method uses the measured intensity of scattered incident light as a function of angle, or phase function. This data can be compared with a phase function calculated from Mie theory to determine particle size, as well as the real and imaginary components of the index of refraction. The accuracy of this technique is estimated as 1%. The second method is based on a resonance spectrum measurement where again scattered light is detected. However, for this method, the scattered light is collected at a fixed angle and the frequency of the incident light is varied. The measured spectrum is again compared with Mie theory to yield particle size and complex index of refraction. The estimated uncertainty of this method is one part in 10^5 . Presently, all particle sizing experiments in this work are performed by measuring the phase function.



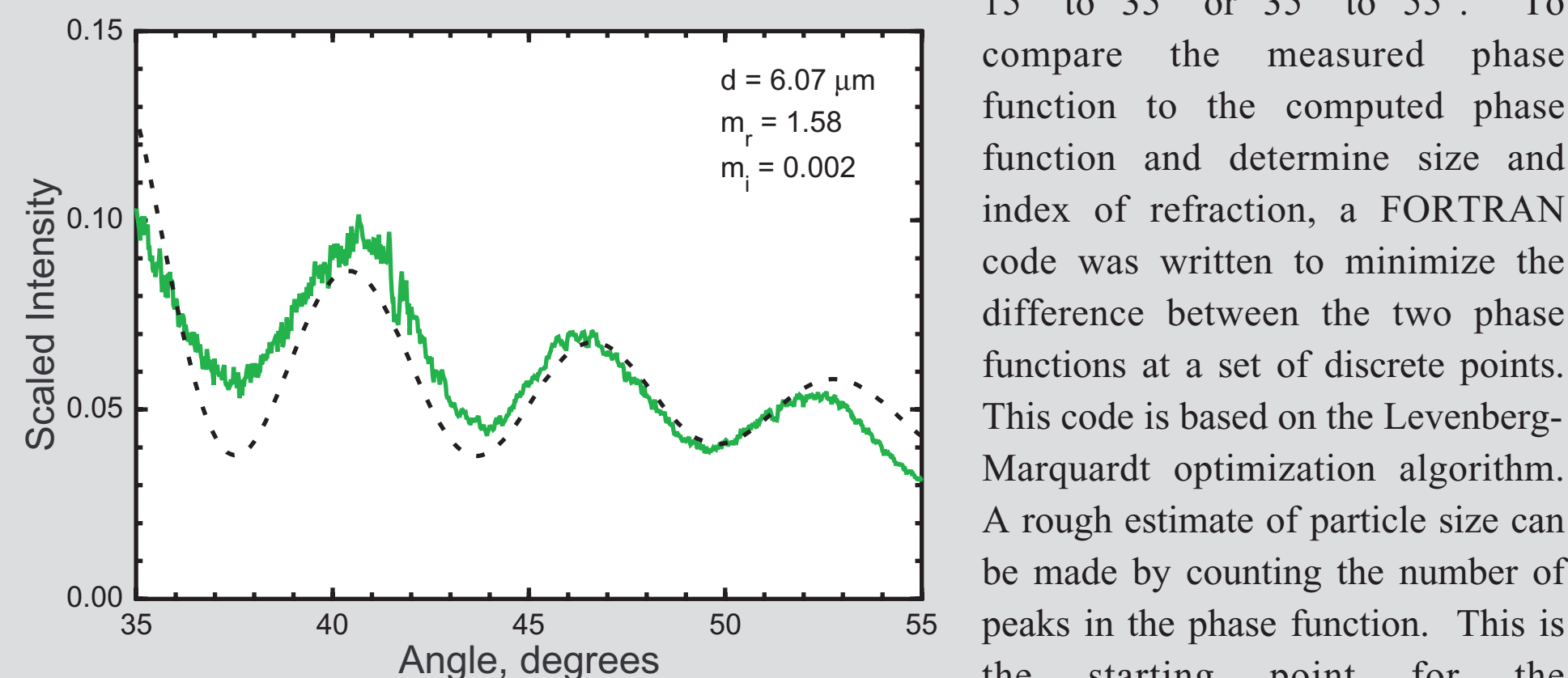
Typical resonance spectrum.

However, for this method, the scattered light is collected at a fixed angle and the frequency of the incident light is varied. The measured spectrum is again compared with Mie theory to yield particle size and complex index of refraction. The estimated uncertainty of this method is one part in 10^5 . Presently, all particle sizing experiments in this work are performed by measuring the phase function.

8

Typical Particle Sizing Results

Typical results for a phase function particle sizing experiment are shown in the figure below. These results are for a 6 μm polystyrene sphere. The incident light source used for particle sizing is a 543.5 nm (green) 0.5 mW laser. The phase function is collected using an uncooled 1024 pixel linear photodetector array. The laser can be positioned to measure angles from either 15° to 35° or 35° to 55°.



Measured and computed phase function for a 6 μm polystyrene sphere.

To compare the measured phase function to the computed phase function and determine size and index of refraction, a FORTRAN code was written to minimize the difference between the two phase functions at a set of discrete points. This code is based on the Levenberg-Marquardt optimization algorithm. A rough estimate of particle size can be made by counting the number of peaks in the phase function. This is the starting point for the optimization.

9

Conclusions

The goal of this work has been to develop diagnostic capabilities to address the largest uncertainties in direct radiative forcing due to aerosols: poorly known scattering efficiencies and absorption cross-sections for typical atmospheric particles. To meet that goal, the following milestones have been achieved:

- An electrodynamic balance facility has been developed to capture and hold single, micrometer sized particles in an electric field. The EDB is capable of levitating both liquid droplets and solid particles. Because the pressure, temperature, and gas composition in the EDB can be controlled, particle experiments in the absence of wall effects can be done over a variety of atmospheric conditions.
- A proof-of-concept experiment has demonstrated that photoacoustic spectroscopy of a single particle can be used to measure energy absorbed by the particle. This technique needs to be further refined to increase signal to noise. A suitable method for calibrating the technique also needs to be developed.
- Particle size and index of refraction have been determined by comparing measured and calculated phase functions.

With further refinement of the diagnostics developed in this work, the EDB facility at Los Alamos National Laboratory will be a versatile tool for an assortment of aerosol experiments.

10

The authors wish to acknowledge Dr. Tim Onasch, BNL, for his assistance with the electrodynamic balance. This work was funded by the DOE Laboratory Directed Research and Development program at Los Alamos National Laboratory.